Selvamarilakshmi D ✉
Prasanna J

https://doi.org/10.21278/TOF.481050923
ISSN 1333-1124
eISSN 1849-1391

EXPERIMENTAL STUDY ON THE EFFECTS OF CROSSBEAM PARAMETERS IN A FIN RAY ROBOTIC GRIPPER IN THE FIELD OF HORTICULTURE APPLICATIONS

Summary

This research introduces an optimal Fin Ray gripper design for vegetable handling in horticulture applications. Fin Ray grippers are triangular with crossbeams. The gripper flexes and adjusts to the structure of the object upon activation. The change in the gripper's form resembles fish fin physiology. This research entails the design and fabrication of Fin Ray inclined grippers with variations in their geometrical structure, namely, the gap between the crossbeams, the inclination angle of the crossbeams, and the thickness of the crossbeams. The Box-Behnken design and analysis of variance approaches were used to assess the major impacts, interactions, and importance of the crossbeam's characteristics on weightlifting capacity and displacement. The Fin Ray gripper design parameters were successfully optimised by the chosen Response Surface Methodology. Less force is needed to obtain a good grasp on an object when a design is made to achieve optimum weightlifting capacity and bending displacement. The gripper's design and analysis, as well as the experimental results demonstrating how well it handles various types of vegetables, are described in the paper. The design of an optimal Fin Ray gripper presents a new and unique idea for adaptive grasping in horticultural robots.

Key words: *Box-Behnken design; crossbeams; Fin Ray gripper; RSM; horticultural robots*

1. Introduction

Soft finger technology has gained significant attention recently, particularly in horticulture applications such as fruit and vegetable harvesting. The use of soft fingers designed to be flexible and compliant has several advantages over conventional grippers, including the ability to handle delicate things without affecting them. Additionally, soft fingers can adapt to irregularly shaped objects, making them ideal for horticultural applications where crops can vary significantly in size and shape. This technology can revolutionise the agriculture industry by reducing labour costs, increasing crop yields, and improving the quality of the produce [1]. Typically, currently available end-effectors are designed to handle specific types of fruits or vegetables that clearly demonstrate their limited versatility when it comes to handling different types [2]. D. Sivanesan and U. Natarajan present a comprehensive overview of soft materials that have been investigated and utilised in high-temperature robotics applications [3].

Several studies have demonstrated the effectiveness of soft fingers for fruit and vegetable harvesting [4]. Soft fingers offer a promising solution to the challenges faced in the horticulture industry. With further developments in soft robotics technology, there is great potential for soft fingers to transform the future of fruit and vegetable harvesting.

The Fin Ray based flexible gripper is one of the most popular soft grippers. A gripper incorporating the Fin Ray effect can offer considerable flexibility and multiple options for grasping products with varying shapes and sizes [5]. Leif Kniese, a scientist, introduced the term "Fin Ray effect" in the late 20th century. The gripper mechanism was designed with inspiration from the structure and movement of a fishtail fin [6]. The Fin Ray gripper has a triangular frame with crossbeams. The gripper moves in the load's direction when it is loaded. The primary aspect of the Fin Ray gripper is its capacity to envelop the objects that are being handled by the robot, hence requiring less force than friction grippers to lift the same object. Additionally, handling brittle and delicate objects is made simpler and safer due to the softness of the gripper.

1.1 Related work

Crooks et al. present a soft robotic gripper designed for use as part of a Tele-operable In-Home Robotic Assistant that is inspired by the Fin Ray effect. The gripper's fingers maximise the effect of a desired bending direction to achieve a stronger and more secure grasp on an object. The gripper is adaptable since it can be made by using various materials utilising 3D printing and can be operated in at least two different ways. Because of the favoured bending direction produced by the Fin Ray effect, the Tele-operable In-Home Robotic Assistant gripper can operate with less force, withstand higher deformations, and support heavier loads, according to experimental testing. The researchers came to the conclusion that the gripper needed to be changed to boost strength and force-exertion capacity while reducing deformation under lateral and torsional loads [7].

Deng and Li [8] proposed learning optimal design parameters for Fin Ray fingers to achieve stable grasping. The task limits are stored as a grouping of the planned gripping force and experimental grasping quality function after learning the pseudo-kinematics of the soft finger in a simulation. Through simulation experiments and real-world examples, the effectiveness of this approach is confirmed. The gripping mechanism of the Fin Ray gripper made of thermoplastic polyurethane (TPU) material has been effectively demonstrated. Research attempts are also being made to design Fin Ray grippers that are suitable for heavy duty and forging applications [9] [10].

Basson et al. [11] proved that the Fin Ray gripper with inclined angle crossbeams of 49.3°, 41.6°, 32.5°, 21.6° and 11.4° produced increased displacement of 14.3% more than the conventional Fin Ray gripper with flat crossbeams.

Elgeneidy et al. [12] studied and explored the effect of inclined grippers. In contrast to the conventional Fin Ray gripper, their conclusion was that the inclusion of angle increments (an angle from 10° to 25° with 3° intervals) between consecutive flexible crossbeams led to an increase of approximately 4 mm in gripper tip displacement along the x-axis and 2 mm along the y-axis towards the grasped object. They also proposed that the gripper’s contact forces after jamming could be greatly increased by structurally modifying the Fin Ray gripper without compromising its inherent passive adaptability to object shapes. A construction that maximises the Fin Ray finger grasping force without harming the object has not yet been discovered.

According to Fu et al., a novel design idea for a variable stiffness gripper (VSG) that is suitable for objects of various sizes and shapes is based on the Fin Ray effect. The proposed design allows for the discrete adjustment of the gripper’s stiffness by changing the orientation of its ribs that can achieve four modes: clamp, hold, pinch, and flex. According to experimental

findings, the VSG can successfully adapt to a variety of objects and change stiffness up to eight times. To accomplish the desired rib orientation, the prototype uses two servo motors that are connected by a belt and pulley system. Additional research will be done to enhance the prototype's performance. This study demonstrates the potential of the VSG based on the Fin Ray effect to significantly improve the capability of robots in grasping tasks. The researchers also advise that additional research be done to enhance the functionality of the VSG by using different materials or adding more ribs [13].

Yang et al. suggest a force-feedback-equipped soft robotic gripper that is lightweight, inexpensive, and simple to operate. It is inspired by the Fin Ray effect and is 3D printed. The gripper's finger structure allows for non-destructive grasping and passive adaptation to conform to the shape of the objects. The gripper is perfect for a variety of uses, including logistical, warehousing, service, intelligent assembly, automatic sorting, and food processing lines. The authors suggest improving on optimising finger size and adding more sensors for position feedback. The proposed gripper could be a valuable addition to the field of soft robotics, where adaptability and flexibility are essential [14].

Bu et al. evaluate the grasp ability of an end-effector using an analytical approach that considers the influence of various parameters such as the dimensions and form of the object being grasped, the contact angle between the Fin Rays and the object, and the number of Fin Rays in contact with the object. The authors demonstrate the effectiveness of their approach by comparing the grasp ability of the Fin Ray end-effector with that of a traditional two-fingered gripper. The findings demonstrate that the Fin Ray end-effector is more suitable for gripping items with uneven forms and surfaces due to its improved grab stability and durability [15].

Based on the literature, it is clear that the three-finger Fin Ray gripper does not cause damage to the object during grasping. Furthermore, a response surface analysis was conducted, revealing the significant impacts of TPU stiffness, grasp distance, and fruit size on the vertical tension of the gripper. Through optimisation, the determined parameters for maximum efficiency are a TPU stiffness of 90HA, a distance of 65 mm, and the use of an apple with a diameter of 84.3 mm [15,16].

Response Surface Methodology (RSM) is a statistical technique used to model and optimise complex systems by investigating the relationship between input variables and a response of interest. RSM provides a systematic and efficient approach to understand the influence of independent variables and identify optimal operating conditions. Experimental designs, such as factorial designs, central composite designs (CCDs, and Box-Behnken designs (BBDs), are commonly used in RSM) [17].

JiSuder et al. present a novel and straightforward approach for assessing the wrapping capacity of the Fin Ray finger structures. The procedure, which was tested using TPU 30D material and a steel roller with a diameter of 20 mm, entails calculating the ratio of the endpoint's deflection to the finger's maximum deflection. The simulation results show that all forms of structures exhibit dependence between individual parameters on the deflection at a constant force. Types of fingers without an interior structure wrap around an object the most. On a few different types of 3D-printed fingers, the simulations were evaluated on actual test equipment before being verified on them. The project's goal was to provide a mechanism for evaluating different structures based on how well they can wrap around an item rather than to identify the best appropriate structure [18].

Fu et al. conclude that their proposed design concept of a VSG based on the Fin Ray effect is effective in achieving adaptive grasping for industrial robots and collaborative robots. The combination of discrete stiffness adjustments and high precision makes it a promising design for various applications. The change in the geometry directly influences the stiffness of the fingers [13].

Md. Ikramul Hasib et al. present an adaptive gripper utilising the Fin Ray effect that provides flexibility for handling products of various shapes. Finite element analysis is used to analyse the displacement of the fin finger caused by the inclination of the crossbeam, resulting in an increased contact surface for grasping objects. Experimental testing demonstrated the effectiveness of the gripper when gripping objects, while the use of a single actuation mechanism simplifies the control system and reduces fabrication costs. The capacity of the gripper can be increased by utilising higher torque stepper motors. The adaptivity of the gripper is also affected by the material of the Fin Ray finger, and the researchers suggest that reducing the thickness of the inclined surface and altering the geometry of the crossbeams could enhance its adaptivity [5].

Flexibility in the Fin Ray finger of a robot gripper refers to the ability of the finger to bend and conform around objects, allowing for effective grasping and manipulation. A flexible Fin Ray finger can adapt to objects of different shapes and sizes, enhancing the gripper's ability to securely hold and lift items. Flexibility directly influences the gripper's weightlifting capacity. A more flexible Fin Ray finger can conform around irregularly shaped objects, increasing the contact area and improving the grip. This enhanced grip can translate into better weightlifting capacity, as the gripper can securely hold objects without slipping or losing control. However, excessive flexibility may result in the finger bending or deforming too much under the weight of the object, causing it to lose grip or not exert enough force to maintain a secure hold. In summary, while flexibility is beneficial for adapting to object shapes, excessive flexibility can indeed reduce the grasping capability of a robot gripper. Striking a balance between flexibility and rigidity, along with considering other design factors, is necessary to optimise the gripper's ability to lift and hold objects securely.

The primary objective of this research is to improve the grip capability of the Fin Ray finger through the optimisation of its crossbeam’s geometry, while maintaining an optimal balance between weightlifting capacity and finger flexibility. Through multiple experiments, the significance of the crossbeam's parameters, including the gap between successive crossbeams, the inclination angle of the crossbeams relative to the gripper's base, and the thickness of the crossbeams, is thoroughly analysed. The results of these experiments successfully verify and validate the impact of these parameters on the gripper's grasping ability when handling vegetables.

2. Design and Analysis

2.1 Fin Ray Finger Design Model

This study presents a two-fingered Fin Ray gripper controlled and actuated by a 5-bar linkage mechanism. To increase the contact area between the objects and the finger, the finger’s inner side width is set at 30 mm and the height and breadth are set at 118.18 mm and 40 mm, respectively. In order to increase the finger grasping ability and to optimise the crossbeam’s geometry of the Fin Ray finger, multiple structures with gaps between the crossbeams of 5 mm, 10 mm, and 15 mm were modelled. The inclination angle of the crossbeams was varied to 90°, 105°, and 120°, and the thickness of the crossbeams was varied between 1.5 mm, 2 mm, and 2.5 mm. The schematic diagram of the grippers with 90° and 120° crossbeam angles is illustrated in Fig. 1.

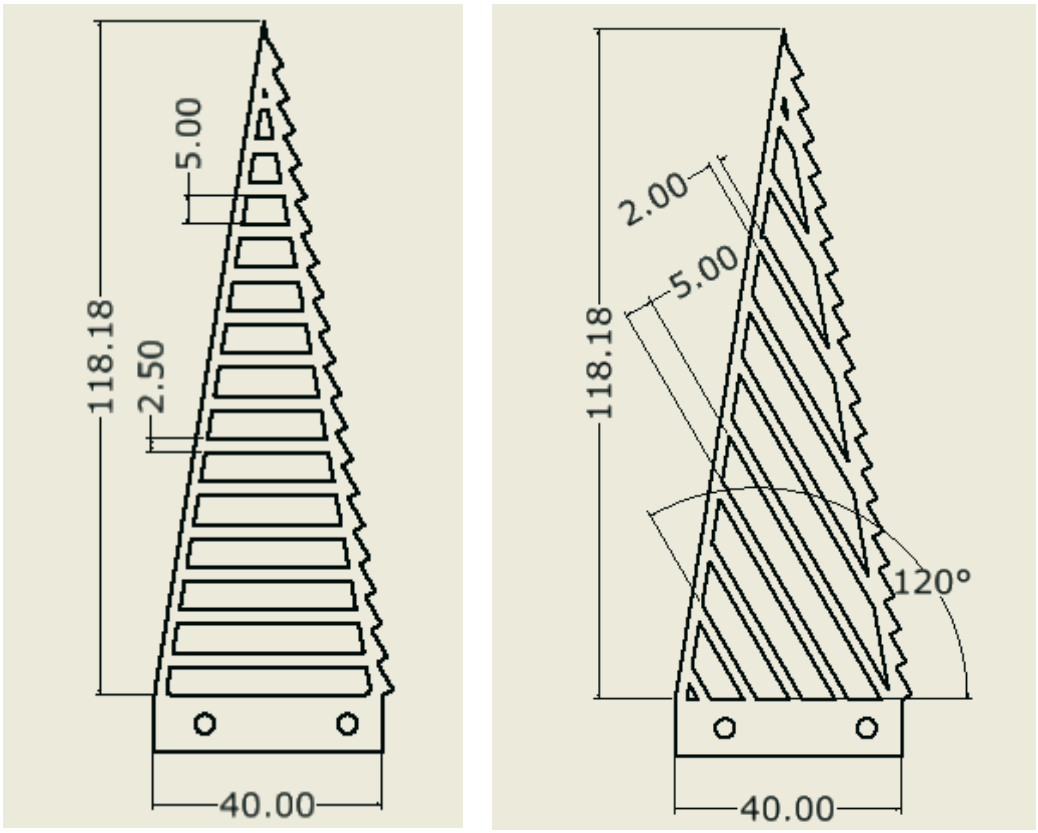

Fig. 1 Schematic diagram of the Fin Ray grippers

The Fin Ray gripper's ridges play an important part in determining how well it can grasp. The finger's surface has raised areas called ridges that increase friction and grip when the gripper makes contact with an object. Additionally, the finger's surface is knurled to improve friction and to aid in object grasping, particularly in the expanded mode. Future studies will look into altering the ridges' properties because the parameters of this study were kept constant.

The Fin Ray finger's ability to grasp objects can be improved by the ridges. The ridges can enhance overall grasping capabilities by adding more points of contact and raising the frictional forces between the gripper and the object. This is especially helpful when handling objects with smooth or slippery surfaces.

The ridges provide better object manipulation and control. The gripper can move more precisely due to the increased surface roughness, which improves dexterity when handling delicate or small objects.

The gripper can be more stable when holding objects due to the ridges. By spreading stresses more equally throughout the contact region, the increased texture can lessen the possibility of slippage or object movement during handling.

For a more stable hold, the ridges can adapt to the shape of the object being grasped. The gripper can adjust to various object shapes and keep a secure grip owing to the Fin Ray finger's flexibility and ridges.

2.2 Stress and Displacement Analysis

The grippers were modelled and analysed using Autodesk Inventor software. Initially, simulations were performed by applying a load of 10 N on the middle of each finger to measure the displacement. The reason for selecting a load of 10 N was to simulate a typical grasping scenario involving objects with weights within the range of 1 kg. Fig. 2 represents the stress and displacement of a flat and inclined gripper when subjected to a load.

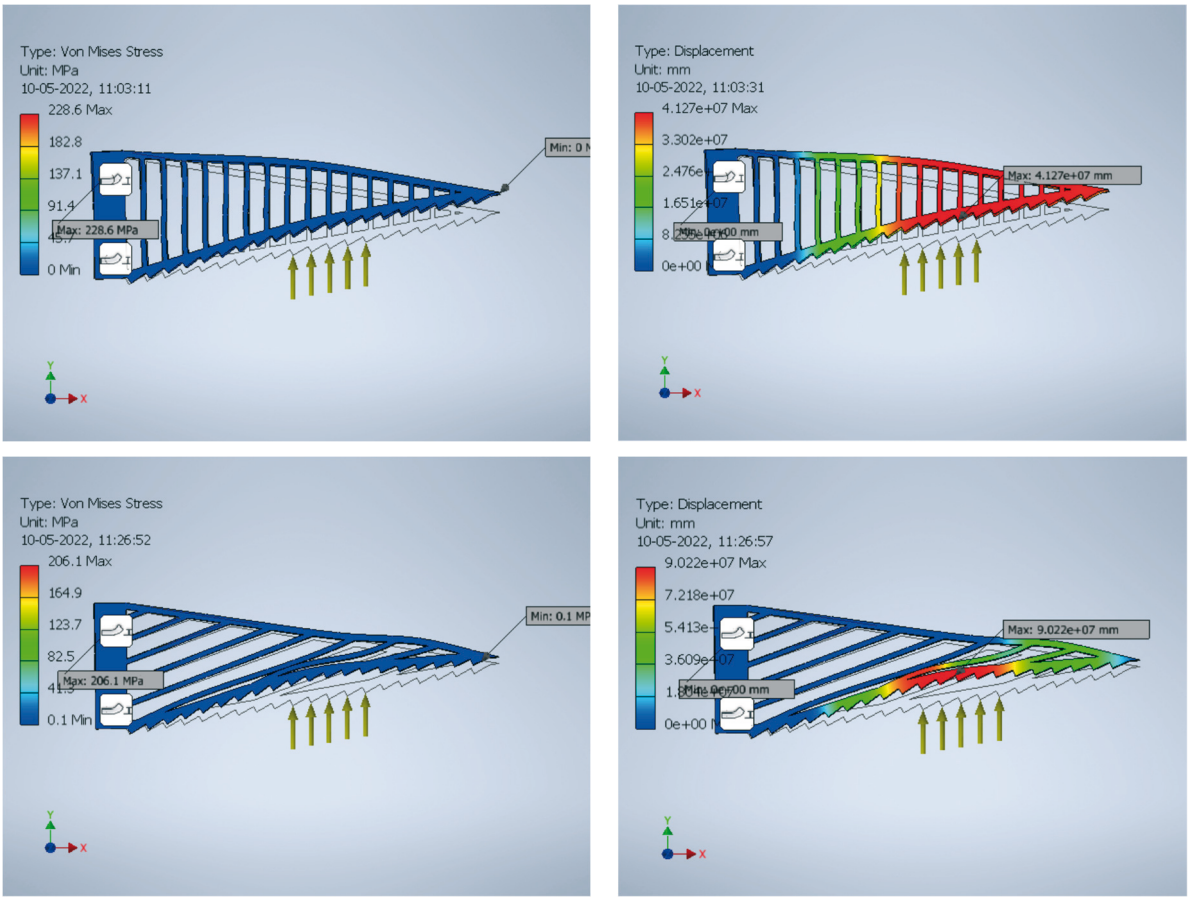

Fig. 2 Simulated stress and displacement of a flat and inclined gripper when subjected to a load.

2.3 Mathematical model

In order to comprehend the phenomenon and estimate the typical forces along the side of the finger in touch with an object, a mathematical model of the Fin Ray effect was created [7].

Figure 3 illustrates the free body diagram (FBD) representing the fundamental structure comprising a base and two crossbeams. In this simplified configuration, a total of four external forces act on the FBD: the applied force and three normal forces at the points where the tip and crossbeams make contact with the object. Employing the method of joints, we derived FBDs for every joint, resulting in ten equations. Additionally, two equations were incorporated to account for the summation of moments on the system. For the purposes of analysis, we will assume the absence of friction, point contact exclusively at the crossbeams, negligible thickness of the members, and the absence of distributed normal force.

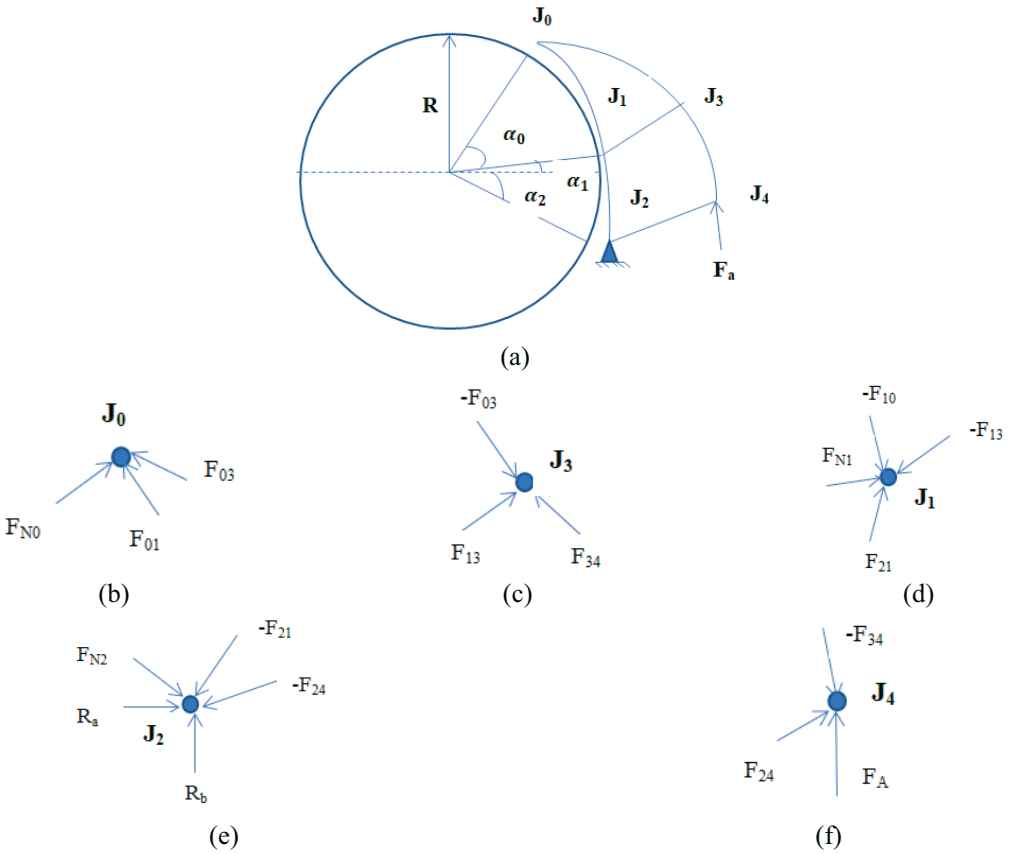

Fig. 3 Free Body Diagram of a Fin Ray finger curling around a circular object

The forces acting on or applied by the tip of the finger can be observed in Figure 3(b), and they can be expressed by the following equations:

$$F_{N0}\cos\alpha_0 + F_{01}\cos x_{01} + F_{03}\cos x_{03} = 0 \tag{1}$$

$$F_{N0}\sin\alpha_0 + F_{01}\sin x_{01} + F_{03}\sin x_{03} = 0\,. \tag{2}$$

In the given context, the angles between Joints 1 and 0 and 0 and 3, relative to the *x*-axis, are denoted as $x_{01}$and x_{03}, respectively. Furthermore, α_0 is defined in Figure 3(a).

The forces acting on or applied by the first crossbeam of the finger can be observed in Figure 3(d), and they can be represented by the following equations:

$$F_{N1}\cos\alpha_1 + F_{01}\cos x_{01} + F_{12}\cos\alpha_{12} + F_{13}\cos x_{13} = 0 \tag{3}$$

$$F_{N1}\sin\alpha_1 + F_{01}\sin x_{01} + F_{12}\sin\alpha_{12} + F_{13}\sin x_{13} = 0, \tag{4}$$

where x_{12} and x_{13} are the angles between Joints 1 and 2 and Joints 1 and 3, respectively, with respect to the *x* axis, and α_1 is defined in Figure3 (a).

The forces exerted on or by the second crossbeam of the finger are shown in Figure 3(b) and are represented by the following equations:

$$F_{N2}\cos\alpha_2 + F_{12}\cos x_{12} + F_{24}\cos x_{24} + R_a = 0 \tag{5}$$

$$F_{N2}\sin\alpha_2 + F_{12}\sin x_{12} + F_{24}\sin x_{24} + R_b = 0, \tag{6}$$

where x_{24} is the angle between Joints 2 and 4 with respect to the *x* axis, and α_2 is defined in Figure 3(a).

AFBD of the third joint is shown in Figure 3(c) and is represented by the following equations:

$$F_{03}\cos x_{03} + F_{34}\cos\alpha_{34} + F_{13}\cos x_{13} = 0 \tag{7}$$

$$F_{03}\sin x_{03} + F_{34}\sin\alpha_{34} + F_{13}\sin x_{13} = 0, \tag{8}$$

where α_{34} is the angle between Joints 3 and 4 with respect to the x axis. AFBD of the third joint is shown in Figure 3(c) and is represented by the following equations:

$$F_{34}\cos x_{34} + F_{24}\cos\alpha_{24} + F_A\cos x_\theta = 0 \tag{9}$$

$$F_{34}\sin x_{34} + F_{24}\sin\alpha_{24} + F_A\sin x_\theta = 0, \tag{10}$$

Where θ is the angle at which F_{applied} is acting on Joint 4 with respect to the x axis:

$$F_{N0}\cos\alpha_0 * l_{0R_a} + F_{N1}\cos\alpha_1 * l_{1R_a} + F_{N2}\cos\alpha_2 * l_{2R_a} - F_{\text{applied}} * l_{24} * \cos\theta = 0 \tag{11}$$

$$F_{N0}\sin\alpha_0 * l_{0R_b} + F_{N1}\sin\alpha_1 * l_{1R_b} + F_{N2}\sin\alpha_2 * l_{2R_b} - F_{\text{applied}} * l_{24} * \sin\theta = 0 \tag{12}$$

2.4 Kinematic Analysis of a Fin Ray gripper

The proposed mechanism consists of five links connected by four revolute joints and one fixed joint. The kinematic analysis of the five-bar mechanism helps in understanding its motion and behaviour when it is subjected to different movements. The dynamic analysis is critical in determining the forces and torques acting on each link of the mechanism and the resulting motion of the mechanism [19].

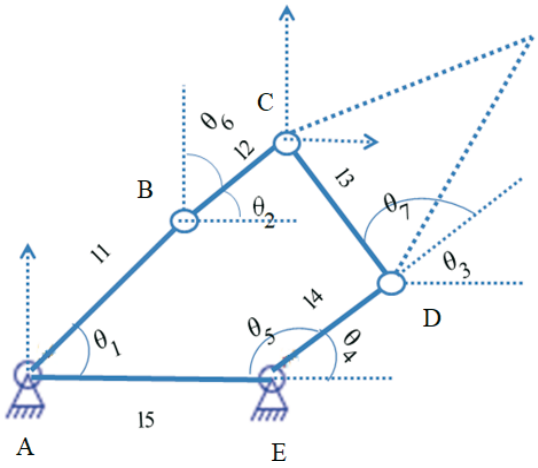

Fig. 4 Schematic diagram of the gripper kinematic model

In order to derive the actuating angles, the following equations are considered. From the coordinate system of the proposed five-bar mechanism, the coordinate of the point C is

$$x_c = l_1\cos\theta_1 + l_2\cos\theta_2 = l_5 + l_4\cos\theta_4 + l_3\cos\theta_3 \tag{13}$$

$$y_c = l_1\sin\theta_1 + l_2\sin\theta_2 = l_3\sin\theta_3 + l_4\sin\theta_4. \tag{14}$$

Here θ_1 and θ_4 are independent. θ_2 and θ_3 can determined by θ_1 and θ_4 as follows:

$$\theta_3 = 2\tan^{-1}\left[\frac{A\pm\sqrt{A^2+B^2-C^2}}{B-C}\right], \tag{15}$$

where

$A=2l_3l_4\sin\theta_4 - 2l_1l_3\cos\theta_1$

$B=2l_3l_5 - 2l_1l_3\cos\theta_1 + 2l_3l_4\cos\theta_4$

$C=l_1^2 - l_2^2 + l_3^2 + l_4^2 + l_5^2 - l_1l_4\sin\theta_1\sin\theta_4 - 2l_1l_5\cos\theta_1 + 2l_4l_5\cos\theta_4 - 2l_1l_4\cos\theta_1\cos\theta_4.$

From Equations (2) and (3) above we get

$$\Theta_2 = \sin^{-1}\left[\frac{l_3\sin\theta_3 + l_4\sin\theta_4 - l_1\sin\theta_1}{l_2}\right]. \quad (16)$$

For effective control, some modifications are required. By combining (13) and (14) and eliminating the secondary angle θ_2 and θ_4, the following equations are obtained:

$$\Theta_1 = 2\tan^{-1}\left[\frac{-B\pm\sqrt{A^2+B^2-C^2}}{-A-C}\right] \quad (17),$$

where $A = x_c;\ B = y_c\ ; C = \frac{l_1^2 - l_2^2 + x_c^2 + y_c^2}{2l_1}$

$$\theta_4 = 2\tan^{-1}\left[\frac{-B\pm\sqrt{A^2+B^2-C^2}}{-A-C}\right], \quad (18)$$

where

$A = x_c - l_5;\ B = y_c;\ C = \frac{l_4^2 + l_5^2 - l_3^2 - 2x_cl_5 + x_c^2 + y_c^2}{2l_4}$.

Equations (17) and (18) allow for direct control of the actuating angles of a mechanism without the need to understand the dependent angles. This is achievable because the equations may be made simpler due to the fixed and known lengths of the links in the mechanism. Consequently, there is only one input needed to control the end-effector's position. In this streamlined way, automating the control of the mechanism is simpler and more convenient than with conventional techniques.

3. Experimental Validation

3.1 Material Properties

The designed grippers were printed using TPU. Polyurethane is a type of plastic that is created in a poly addition reaction when diisocyanate interacts with one or more diols. To be risk free in human interaction, TPU material with a lower Young's modulus than silicone was preferred in the fabrication of flexible and adaptable soft robotic grippers. The TPU material is used as a soft technical plastic or a hard rubber replacement. Because of the TPU's high shear strength, elasticity, and flexibility, the grippers were printed with TPU of 90A shore hardness to obtain good flexibility without sacrificing gripper strength [15]. Further, TPU was chosen for its capacity to absorb additional shocks while having sufficient flexibility to adapt to the handled object.

3.2 Fabrication Method

The chosen manufacturing approach for producing the required components was rapid prototyping using a plastic deposition. A customised Prusa-I3 3D-printing system and a UP 3D-printing system were used to create the parts and build up the part from the base plate, where plastic is placed layer by layer. For the 3D print to be exactly aligned for each layer, the printing bed must be calibrated. The layer thickness was 0.3 mm, with appendages having a density of 100% and gripper components a density of 60%. The bed temperatures were set ranging from

200 to 250 degrees Celsius, depending on the print medium used. The fingers were employed throughout the experiment and were put to the test for compliance.

In order to control and actuate the gripper, a 5-bar linkage mechanism was developed and fabricated. The motor that actuates the opening and closing of the gripper was controlled by a microcontroller. The Fin Ray gripper setup was then mounted onto the wrist of a 6-axis articulated robot, which is shown in Fig. 6. Force Sensing Resistors were attached to the grasping sides of the fingers to measure the force of the finger. The robotic arm was programmed according to the path described for experimental runs through lead-through programming. The gripper was tested to determine how much weight it could lift and how far it could move while holding vegetables of varying sizes up to a maximum diameter of 80 mm.

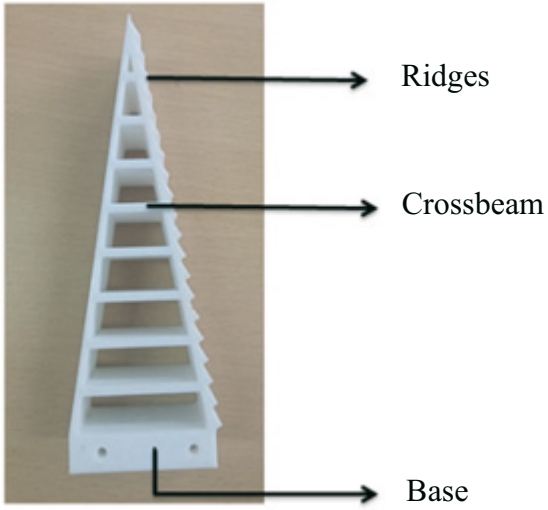

Fig. 5 Fin Ray Gripper - Physical model

Fig. 6 Developed gripper attached to an industrial robot

3.3 Experimentation

Figure 7(a) shows an optimal Fin Ray gripper handling cylinder and spherical and oval shaped objects. Figure 7(b) shows an optimal Fin Ray gripper handling a capsicum, tomato, and potato. Multiple objects with variable sizes were successfully grasped using the proposed gripper. In our experimental study, we focused on measuring the weightlifting capacity of the gripper during object grasping. To achieve this, we employed a methodology that involved selecting objects with the same shape but varying weights. By doing so, we were able to isolate the weight as the primary variable of interest while maintaining consistent grasping conditions. Through this approach, we successfully identified and quantified the gripper's weight-carrying capacity. In addition to measuring the weightlifting capacity, we also manually measured the finger bending displacement during the gripping process. This involved observing and recording the extent to which the gripper's fingers flexed or bent when grasping the objects. By monitoring the finger bending displacement, we obtained valuable information on the gripper's flexibility and its ability to adapt to different object shapes and sizes. This manual measurement process allowed us to assess the gripper's dexterity and understand how it responded to the grasping forces applied during weightlifting. After measuring the weightlifting capacity and finger bending displacement of the gripper, we employed response surface methodology (RSM) to identify the optimal configuration for the Fin Ray gripper. RSM is a statistical technique used to model and optimise complex systems by analysing the relationships between input variables and output responses.

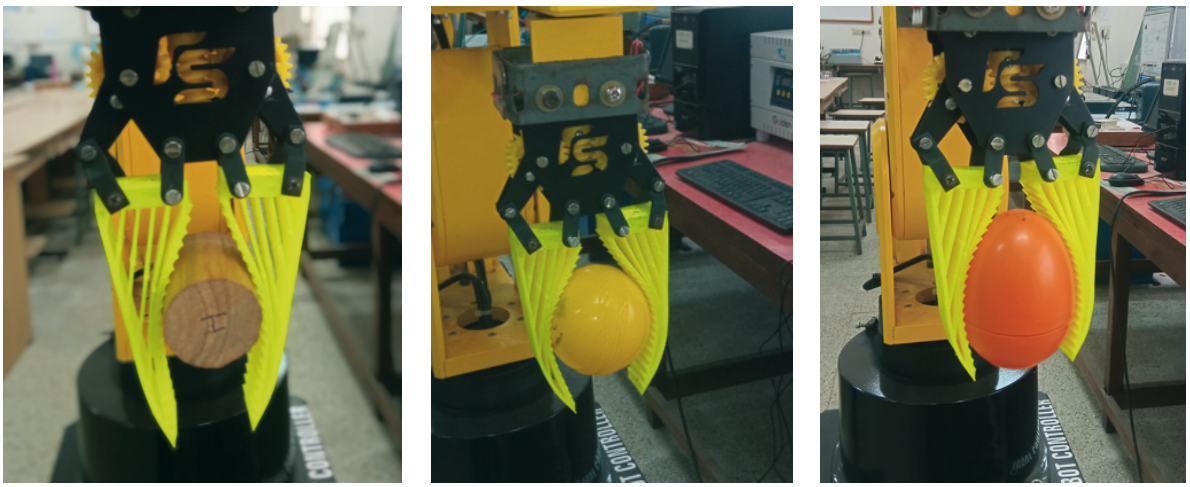

(a)

(b)

Fig. 7 (a) Optimal Fin Ray gripper handling three different shapes of objects (b) Optimal Fin Ray gripper handling a capsicum, tomato and potato

3.4 Force Measurement

Fig. 8 Force-Sensing Resistors (FSR)

Force-Sensing Resistors (FSR) are employed in Fin Ray fingers to enable them to sense and adjust the force exerted during grasping and object manipulation. By integrating FSR sensors into the contact surfaces of the fingers, the robotic hand can detect the force applied to its fingertips or along the length of the finger.

The FSR sensors in Fin Ray fingers work by measuring the changes in electrical resistance caused by the applied force. As pressure is exerted on the sensor, the conductive particles within the FSR material come into closer contact, leading to a decrease in resistance. The change in resistance is proportional to the force being applied, allowing for accurate force detection [20].

FSR sensors exhibit a logarithmic response to force. Initially, as a small force is applied, the voltage output remains relatively low. As the force increases, the voltage output starts to rise more rapidly. At a certain point, known as the threshold force, the FSR reaches its maximum sensitivity and the voltage output begins to saturate, meaning that further increases in force may not result in significant changes in voltage.

FSR sensors were used on the fingers, and this setup was interfaced with Arduino to calculate the forces involved in the gripping operation.

The FSR analogue readings were captured using an Arduino and a 10k resistor to determine the pressure of the gripping force. This value corresponds to the force exerted on the FSR while holding an object, allowing for force measurements. When an FSR is attached to a Fin Ray finger, the applied force vs voltage values can be noted. These values represent the relationship between the amount of force applied to the Fin Ray finger and the corresponding voltage output from the FSR. By measuring and recording these values, it becomes possible to analyse and understand the force-sensing capabilities of the Fin Ray finger.

The graph below illustrates the correlation between the applied force and voltage of the FSR. It visually represents how the voltage output of the FSR changes in response to varying levels of applied force.

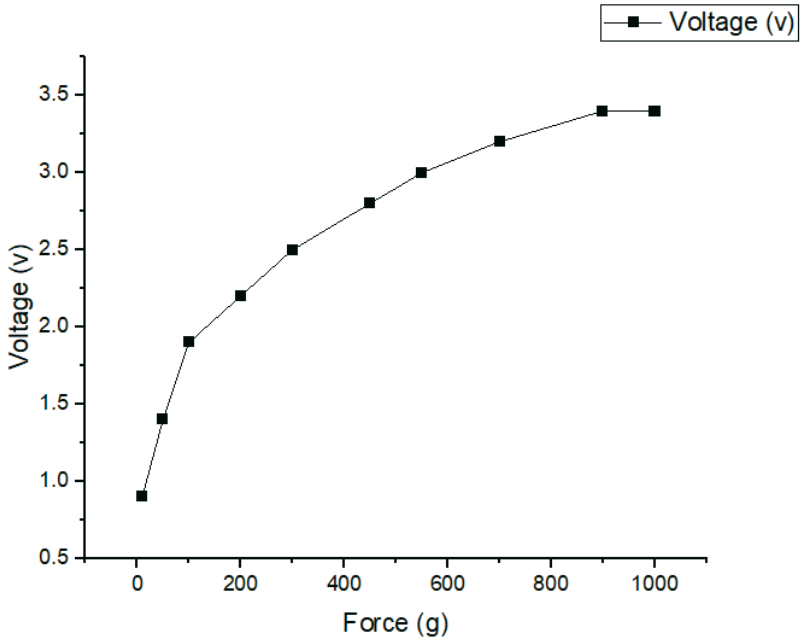

Fig. 9 Voltage vs. Force

3.5 Box-Behnken Modelling

Response Surface Methodology (RSM) is a collection of statistical and mathematical tools that determine the relationship between input and output characteristics. The experimental runs are performed using the Box-Behnken design that is a type of RSM experimental design formulated by George Box and Donald Behnken in 1960. Box-Behnken designs are used to produce higher order response surfaces with fewer runs than a full factorial design. RSM reveals the extent of nonlinearity and the effect of parameter interaction in the investigated process, allowing the best and most efficient designs for the chosen application [21].

The factors under consideration were the gap between the crossbeams, the inclination angle of the crossbeams, and the thickness of the crossbeams. The responses evaluated in the Fin Ray gripper were the weightlifting capacity and the gripper's tip displacement.

Design Expert 13 statistical software was used to create and analyse the design. In this method, each crossbeam factor was equally spaced by three-coded values named -1, 0, and +1. The levels of the input parameters are displayed in Table 1. The detailed experimental runs with uncoded values of crossbeam parameters and the corresponding responses are presented in Table 2.

Table 1 Ranges for Experiments and Independent Variables.

Design Variables	Factors	Range and levels		
X_1	Crossbeam gap /mm	1.5	2	2.5
X_2	Inclination angle of the crossbeam /°	90	105	110
X_3	Crossbeam thickness /mm	5	10	15

Table 2 Box-Behnken Design with Experimental Values for the Independent Variable.

Crossbeam Gap /mm	Inclination Angle of the crossbeam /°	Crossbeam Thickness /mm	Weightlifting Capacity /N	Displacement /mm
X_1	X_2	X_3	Y_1	Y_2
15	90	2	4.12	16
10	105	2	21.08	8
10	105	2	20.89	8
10	90	1.5	8.83	12
10	105	2	20.79	8
15	120	2	3.43	17
10	120	1.5	10.79	13
5	120	2	13.73	9
10	90	2.5	15.69	5
5	105	1.5	4.90	11
15	105	1.5	1.18	18
5	90	2	8.34	4
10	120	2.5	19.61	10
10	105	2	20.59	8
15	105	2.5	5.88	15
5	105	2.5	16.67	3
10	105	2	20.79	8

The mathematical expression that correlates the process parameters and performance characteristics was a second-order polynomial regression equation. The required quadratic model is described by

$$Y_i = \beta_0 + \beta_1 X_{i1} + \beta_2 X_{i2} + \beta_3 X_{i3} + \beta_{11} X_{i1}^2 + \beta_{22} X_{i2}^2 + \beta_{33} X_{i3}^2 + \beta_{12} X_{i1} X_{i2} + \beta_{12} X_{i1} X_{i3} + \beta_{23} X_{i2} X_{i3} + \varepsilon_i, \quad (19)$$

where Y is a response variable, β represents a set of regression coefficients, and ε is an unknown constant error vector [22,23].

Table 2 shows that the crossbeam gap of 10 mm had the highest weightlifting capacity when compared with the others. When compared with other combinations, the combination of crossbeam gap, crossbeam inclination angle, and crossbeam thickness of 10 mm, 105°, and 2 mm yields good results as it provides a larger encompassing area with moderate stiffness. By estimating the regression equation and analysing the response of the response surface and contour plots, the optimal setting of the crossbeam parameters was identified [24].

4. Results and Discussion

The analysis of variance (ANOVA) results are shown in Table 3. Equations 2 and 3 represent the mathematical modelling for weightlifting capacity and displacement, respectively.

According to the ANOVA statistical analysis, the quadratic models of weightlifting capacity and displacement are statistically significant and accurately fit the process parameters.

The effect of the parameters is considered significant when the p value is lower or equal to 0.05 (95% confidence level).

Table 3 ANOVA for the Response Surface Quadratic Model.

Source	Y_1- Weightlifting Capacity				Y_2- Displacement			
	Sum of Squares	**Mean Square**	***F*- value**	***p*-value**	**Sum of Squares**	**Mean Square**	***F*-value**	***p*-value**
Model	840.71	93.41	1725.50	<0.0001	318.22	35.36	990.02	<0.0001
X_1	105.34	105.34	1945.87	<0.0001	190.12	190.12	5323.50	<0.0001
X_2	13.99	13.99	258.46	<0.0001	18.00	18.00	504.00	<0.0001
X_3	129.20	129.20	2386.62	<0.0001	55.13	55.13	1543.50	<0.0001
X_1X_2	9.24	9.24	170.71	<0.0001	4.00	4.00	112.00	<0.0001
X_1X_3	12.50	12.50	230.83	<0.0001	6.25	6.25	175.00	<0.0001
X_2X_3	0.9604	0.9604	17.74	0.0040	4.00	4.00	112.00	<0.0001
X_1^2	420.86	420.86	7774.12	<0.0001	29.01	29.01	812.37	<0.0001
X_2^2	49.40	49.40	912.50	<0.0001	3.22	3.22	90.26	<0.0001
X_3^2	56.80	56.80	1049.13	<0.0001	5.33	5.33	149.21	<0.0001
Residual	0.3790	0.0541			0.2500	0.0357		
Lack of Fit	0.2521	0.0840	2.65	0.1850	0.2500	0.0833		
Pure Error	0.1269	0.0317			0.0000	0.0000		
Cor Total	841.09				318.47			

The robustness of the model was evaluated using both the coefficient of determination (R^2) and the adjusted coefficient of determination (adjusted R^2) for weightlifting capacity and displacement. They were both found to be greater than 0.999 for both responses. Since the values are very close to 1, the models were proven to be efficient.

The mathematical models were used to predict the responses. They are shown below:

$$Y_1 = -285.5392 + 10.8144X_1 + 3.3571X_2 + 67.0115X_3 - 0.0203X_1X_2 - 0.707000X_1X_3 + 0.0653X_2X_3 - 0.3999X_1^2 - 0.0152X_2^2 - 14.6910\,X_3^2 \quad (20)$$

(R^2 = 0.9995, Adj. R^2 = 0.9990 and Pred. R^2= 0.9950)

$$Y_2 = 93.625 - 0.725X_1 - 0.85X_2 - 42.25X_3 - 0.0133X_1X_2 + 0.5X_1X_3 + 0.133333X_2X_3 + 0.105\,X_1{}^2 + 0.0039\,X_2{}^2 + 4.5\,X_3{}^2 \quad (21)$$

(R^2=0.9992, Adj. R^2 =0.9982 and Pred. R^2= 0.9874.)

Fig. 7 illustrates the normal probability plot of the residuals for weightlifting capacity and displacement. It can be observed that the residuals are clustered about a straight line that proves the validity of the model assumptions and indicates that errors are distributed normally.

The results of the ANOVA show that crossbeam thickness (C) is the most significant parameter that significantly affects the weightlifting capacity of the robotic arm fitted with the Fin Ray gripper, followed by the crossbeam gap and the inclination angle of the crossbeam. It can also be learnt that the interactions among the crossbeam parameters have a significant impact on the weightlifting capacity. The response surface plots are illustrated in Fig. 8.

(a)

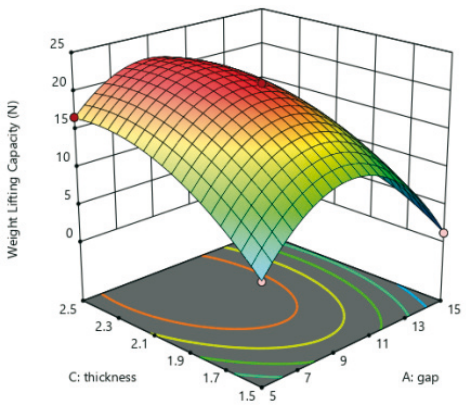

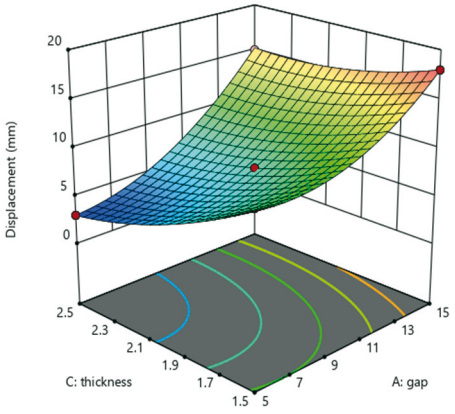

(b)

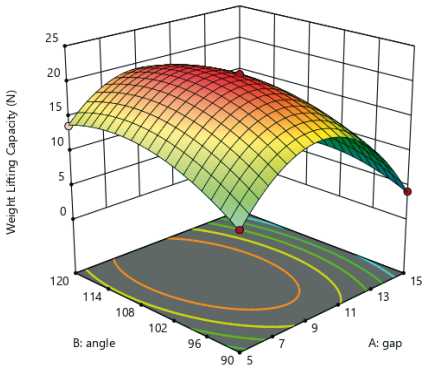

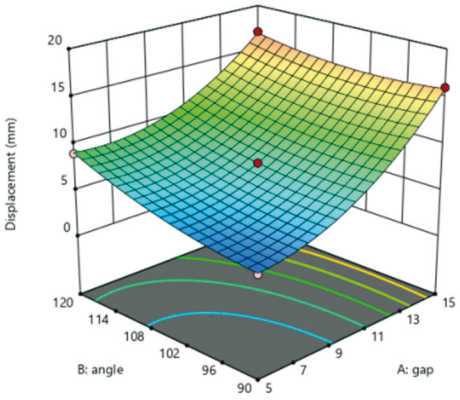

(c)

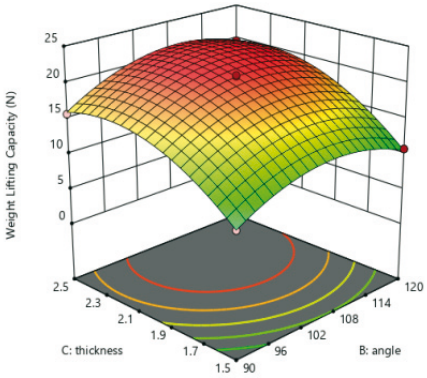

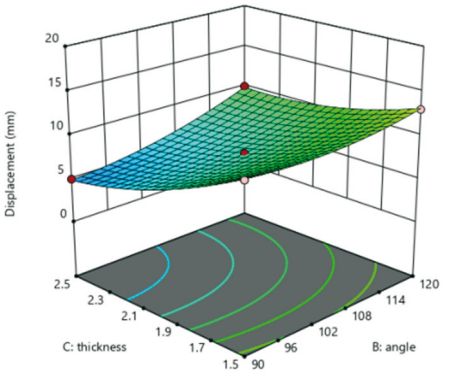

Fig. 10 (a) Response surface plot for the effects of gap and thickness on the responses; (b) Response surface plot for the effects of angle and gap on the responses; (c) Response surface plot for the effects of angle and thickness of the responses.

From Fig. 10(a), it can be observed that a crossbeam thickness of 1.5 mm exhibits a high displacement of 18 mm. The reason is that the gripper is more flexible and has low rigidity, which makes it offer a very low weightlifting capacity. When the crossbeam thickness is increased from 1.5 to 2.5 mm, the displacement of the gripper is reduced, indicating an increase in stiffness. However, it is found that a crossbeam thickness of 2 mm was established as an optimal setting that provides high weightlifting capacity (20.79 N). This optimal setting with moderate displacement (8 mm) tends to increase the area of contact between the gripper and the object without compromising rigidity. The crossbeam gap (A) is the second most important parameter influencing weightlifting capacity. When the space between the crossbeams is increased to 15 mm, the robot's ability to lift weight is significantly reduced when compared with the other two settings. This is because increasing the gap between the crossbeams substantially reduces the gripper's stiffness. The interaction setting A2 × C2 that provides moderate displacement and stiffness has a notable impact on load-carrying capacity.

Fig. 10(b) shows that the increase in the inclination angle of the crossbeam from 90° to 120° increases the displacement from 4 to 9 mm, respectively. This indicates that the increase in the inclination angle of the crossbeam augments the flexibility of the gripper [4] that lessens the strength and rigidity of the finger. The interaction setting A2 × B2 has a synergistic effect on enhancing the weightlifting capacity. This setting provided a strong weightlifting capacity of 20.5 N. The reason is that better flexibility in encompassing the spherical object is achieved through the inclination angle of 105°, and effective stiffness is offered by the medium crossbeam gap of 10 mm. As expected, the interaction setting B2 × C2 (inclination angle of 105° and crossbeam thickness of 2 mm) is optimal for better weightlifting capacity that can be visualised in Fig. 10(c). From the mathematical model, the optimal setting of the gripper parameters for better weightlifting capacity (21.08 N) is found to be 10 mm of the crossbeam gap, 105° of the inclination angle, and 2 mm of the crossbeam thickness.

5. CONCLUSION

The construction of the Fin Ray gripper was modified by varying the gap between the crossbeams, the inclination of the crossbeam angle, and the crossbeam thickness. The effects of the crossbeam parameters on the gripping efficiency of the Fin Ray gripper were experimentally investigated on a 6-axis articulated robot while handling vegetables. Weightlifting capacity and displacement of the gripper were evaluated to analyse the grasping ability. The following conclusions were drawn based on the experimental results obtained through the Box-Behnken method and the statistical analysis of ANOVA.

1. Wide crossbeam gaps (15 mm), a larger inclination angle (120°), and less crossbeam thickness (1.5 mm) create larger displacements of 18 mm, which implies more flexibility and less stiffness of the gripper. Hence, this setting offered very low weightlifting capacity.
2. A small crossbeam gap of 5 mm, a lower inclination angle of 90°, and a crossbeam thickness of 2.5 mm give more rigidity to the gripper, which leads to low flexibility. This makes the Fin Ray gripper behave as a flat gripper, where there are fewer contact points between the gripper and the object. Therefore, this design of the gripper also provided a low weightlifting capacity.
3. The crossbeam parameters of a 10 mm gap between the crossbeams, a 105° inclination angle, and a 2 mm crossbeam thickness provide moderate displacement of 8 mm with a high weightlifting capacity of 21.08 N. This setting was confirmed as the optimal setting for better weightlifting capacity. This is because the moderate displacement of the gripper provides suitable flexibility that aids the gripper in encompassing the object, which improves the weightlifting capacity.
4. For higher weightlifting capacity, the ideal condition necessitates moderate flexibility without sacrificing the rigidity of the gripper.
5. The quadratic models arrived at by using the Box-Behnken experimental design have a very high coefficient of determination (R^2 of 0.9990 for weightlifting capacity and 0.9982 for displacement) and are therefore accurate.
6. According to the results of ANOVA, the crossbeam parameters that were selected to evaluate and enhance the effectiveness of the Fin Ray gripper proved to be highly significant.

In conclusion, the optimisation of the Fin Ray gripper's finger design through RSM resulted in an optimal configuration that exhibits high weightlifting capacity. This high

weightlifting capacity is closely tied to the finger's grasping ability, which is greatly influenced by its flexibility. By optimising the geometry of the Fin Ray finger, its gripping ability was significantly enhanced, enabling it to handle a wide variety of items effectively. This technique has significant uses in horticulture, including lower labour costs, higher crop yields, and better produce quality. In order to construct a highly effective and precise system that has the potential to alter the agricultural sector, we intend to incorporate the improved finger design into a harvesting robot. By showcasing the capabilities of Fin Ray gripper technology, we hope to open the door for further advancements in automation and robotics.

REFERENCES

[1] Eduardo Navas, Roemi Fernández, Delia Sepúlveda, Manuel Armada and Pablo Gonzalez-de-Santos, "Soft Grippers for Automatic Crop Harvesting: A Review", Sensors, 2021, pp-1-27. https://doi.org/10.3390/s21082689

[2] Ziyue Li, Xianju Yuan and Chuyan Wang, "A review on structural development and recognition-localization methods for end-effector of fruit-vegetable picking robots", International Journal of Advanced Robotic Systems, 2022, pp-1-29

[3] Desingh Sivanesan , Uthirapathy Natarajan and Veeramalai Chinnasamy Sathish Gandhi, "Experimental and Finite Element Studies of a Soft Robot Finger Material - a Contact Mechanics Approach," Transactions of Famena, 2018, pp. 75-84. https://doi.org/10.21278/TOF.42407

[4] Jongpyo Jun, Jeongin Kim, Jaehwi Seol, Jeongeun Kim and Hyoung Il Son, "Towards an Efficient Tomato Harvesting Robot:3D Perception, Manipulation, and End-Effector", IEEE access, 2021, pp- 17631- 17640. https://doi.org/10.1109/ACCESS.2021.3052240

[5] Md. Ikramul Hasib, Md. Helal An Nahiyan, Fahim Islam Anik, Md Jarir Hossain, Md. Najmus Salehin, "Development of an Adaptive Gripper with Fin-Ray effect", International Conference on Mechanical, Industrial and Materials Engineering, 2019, pp-505-510

[6] O. Pfaff, S. Simeonov, I. Cirovic and P. Stano, "Application of fin ray effect approach for production process automation," Ann. DAAAM Proc., vol. 22, no. 1, pp. 1247-1249, 2011. https://doi.org/10.2507/22nd.daaam.proceedings.608

[7] Whitney Crooks, Gabrielle Vukasin, Maeve O'Sullivan, William Messner and Chris Rogers, "Fin Ray® effect inspired soft robotic gripper", Frontiers Robotics AI. 3 (2016), pp1-9. https://doi.org/10.3389/frobt.2016.00070

[8] Zhifeng Deng and Miao Li, "Learning optimal fin-ray finger design for soft grasping," Front. Robot. AI, pp. 161, 2021. https://doi.org/10.3389/frobt.2020.590076

[9] A. Müller, M. Aydemir, A. Glodde, and F. Dietrich, "Design Approach for Heavy-Duty Soft-Robotic-Gripper," Procedia CIRP, vol. 91, pp. 301-305, 2020. https://doi.org/10.1016/j.procir.2020.02.180

[10] Caner-VeliInce, Jan Geggiera and Annika Raatza,"Fin Ray gripper for handling of high temperature hybrid forging objects," Procedia CIRP 106, pp.114-119, 2022. https://doi.org/10.1016/j.procir.2022.02.164

[11] C. I. Basson, G. Bright, and A. J. Walker, "Analysis of flexible end-effector for geometric conformity in reconfigurable assembly systems: testing geometric structure of grasping mechanism for object adaptibility," in 2017 Pattern Recognition Association of South Africa and Robotics and Mechatronics (PRASA-RobMech), 2017, pp. 92-97. https://doi.org/10.1109/RoboMech.2017.8261129

[12] Khaled Elgeneidy, Adel Fansa, Irfan Hussain, Khaled Goher, "Structural Optimization of Adaptive Soft Fin Ray Fingers with Variable Stiffening Capability" ,3rd IEEE International Conference on Soft Robotics (RoboSoft), 2020. https://doi.org/10.1109/RoboSoft48309.2020.9115969

[13] Jiaming Fu1, Han Lin, I.V.S Prathyush, Xiaotong Huang, Lianxi Zheng, and Dongming Gan, "A Novel Discrete Variable Stiffness Gripper Based on the Fin Ray Effect", Intelligent Robotics and Applications, 2022, (pp.791-802). https://doi.org/10.1007/978-3-031-13835-5_71

[14] Yang Yang, Kaixiang Jin, Honghui Zhu, Gongfei Song, Haojian Lu and Long Kang, "A 3D-Printed Fin Ray Effect Inspired Soft Robotic Gripper with Force Feedback", Micromachines,2021, pp.1-14. https://doi.org/10.3390/mi12101141

[15] Lingxin Bu, Guangrui Hu and Jun Chen, "Assessment of Grasp Ability for An End-effecter with Fin-ray Structure", Journal of Physics: Conference Series, 2021, pp1-10

[16] LingXin Bu, ChengKun Chen, GuangRui Hu, JianGuo Zhou, AdiletSugirbay, Jun Chen ,ASSESSMENT OF APPLE DAMAGE CAUSED BY A FLEXIBLE END-EFFECTOR, INMATEH -Agricultural Engineering,2021,pp.309-316. https://doi.org/10.35633/inmateh-62-32

[17] Noor basha Zeelanbasha, Vellimalai Senthil and Bella Raman Senthil Kumar, "An Integrated Approach of RSM and MOGA for the Prediction of Temperature Rise and Surface Roughness in the End Milling of Al 6061-T6", Transactions of Famena, 2018, pp. 115-128. https://doi.org/10.21278/TOF.42308

[18] Jiří Suder, Zdenko Bobovský, Jakub Mlotek , Michal Vocetka, Petr Oščádal and Zdeněk Zeman, "Structural Optimization Method of a FinRay Finger for the Best Wrapping of Object", Applied Sciences, 2021, pp.1-18. https://doi.org/10.3390/app11093858

[19] Bin Zi, Jianbin Cao and Zhencai Zhu, "Dynamic Simulation of Hybrid-Driven Planar Five-bar Parallel Mechanism Based on SimMechanics and Tracking Control,"Int J Adv Robotic Sy, 2011, Vol. 8, No. 4, 28-33. https://doi.org/10.5772/45683

[20] Jun Liu, Jiandang Xing, Xiaodong Ruan, Jian Song and Di Wu, "Analysis and Design of the Reconfiguration Motion Qualities of a Deformable Robot Based on a Metamorphic Mechanism", Transactions of Famena, 2023, pp. 79-97. https://doi.org/10.21278/TOF.472043022

[21] A. Ramesh Kumar, S. Jayabal, M. Pradeep Kumar, P. Thirumal, "A Qualitative Analysis of Indoor Air Quality Pollutants inside a Private Car Cabin Using Response Surface Methodology", Transactions of Famena, 2022, pp.41-55. https://doi.org/10.21278/TOF.461017020

[22] Mustafa Agah Tekindal, Hülya Bayrak, Berrin Özkaya, Yasemin Yavuz," Second-order response surface method: factorial experiments an alternative method in the field of agronomy", Turkish Journal of Field Crops, 2014, pp. 35-45. https://doi.org/10.17557/tjfc.78787

[23] Ijomah Maxwell Azubuike," Second Order Regression with Two Predictor Variables Centered on Mean in an Ill Conditioned Model", International Journal of Statistics and Applications 2019, 101-110

[24] C. Selvan and S. R. Balasundaram, "Data Analysis in Context-Based Statistical Modeling in Predictive Analytics," in Handbook of Research on Engineering, Business, and Healthcare Applications of Data Science and Analytics, IGI Global, 2021, pp. 96-114. https://doi.org/10.4018/978-1-7998-3053-5.ch006

Submitted: 15.02.2023

Accepted: 24.7.2023

Selvamarilakshmi D*
Prasanna J
Department of Mechanical Engineering, College of Engineering Guindy, Anna University, Chennai, India
*Corresponding author:
selvamoorthy08@gmail.com